High pressure oxidation of C_2H_4/NO mixtures

J. Giménez-López[1,2], M.U. Alzueta[2], C.T. Rasmussen[1], P. Marshall[3], P. Glarborg[1]

[1] Department of Chemical and Biochemical Engineering, Technical University of Denmark, Lyngby (Denmark).

[2] Aragón Institute of Engineering Research (I3A), University of Zaragoza, Zaragoza (Spain).

[3]Department of Chemistry and Center for Advanced Scientific Computing and Modeling (CASCaM), University of North Texas, Denton, Texas

CORRESPONDING AUTHOR
Peter Glarborg, Department of Chemical and Biochemical Engineering, Technical University of Denmark, DK-2800 Lyngby, Denmark
Email: pgl@kt.dtu.dk
Tel: +45 4525 2957
Fax: +45 4588 2258

WORD COUNT: well below 6000 words

High pressure oxidation of C_2H_4/NO mixtures

J. Giménez-López[1,2], M.U. Alzueta[2], C.L. Rasmussen[1], P. Marshall[3], P. Glarborg[1]

[1] Department of Chemical and Biochemical Engineering, Technical University of Denmark, Lyngby (Denmark).

[2] Aragón Institute of Engineering Research (I3A), University of Zaragoza, Zaragoza (Spain).

[3]Department of Chemistry and Center for Advanced Scientific Computing and Modeling (CASCaM), University of North Texas, Denton, Texas

Abstract

An experimental and kinetic modeling study of the interaction between C_2H_4 and NO has been performed under flow reactor conditions in the intermediate temperature range (600-900 K), high pressure (60 bar), and for stoichiometries ranging from reducing to oxidizing conditions. The main reaction pathways of the $C_2H_4/O_2/NO_x$ conversion, the capacity of C_2H_4 to remove NO, and the influence of the presence of NO_x on the C_2H_4 oxidation are analyzed. Compared to the C_2H_4/O_2 system, the presence of NO_x shifts the onset of reaction 75-150 K to lower temperatures. The mechanism of sensitization involves the reaction $HOCH_2CH_2OO + NO \rightarrow CH_2OH + CH_2O + NO_2$, which pushes a complex system of partial equilibria towards products. This is a confirmation of the findings of Doughty et al. [*Proc. Combust. Inst.* 26 (1996) 589-596] for a similar system at atmospheric pressure. Under reducing conditions and temperatures above 700 K, a significant fraction of the NO_x is removed. This removal is partly explained by the reaction $C_2H_3 + NO \rightarrow HCN + CH_2O$. However, a second removal mechanism is active in the 700-850 K range, which is not captured by the chemical kinetic model. With the present thermochemistry and kinetics, neither formation of nitro-hydrocarbons (CH_3NO_2, $C_2H_3NO_2$, $C_2H_5NO_2$, $CHOCH_2NO_2$) nor nitroso-compounds (CH_3NO, C_2H_3NO, C_2H_5NO, $ONCH_2CHO$, $CH_3C(O)NO$, $ONCH_2CH_2OH$) contribute to remove NO_x.

Introduction

Ethylene is an important intermediate in the combustion of most hydrocarbon fuels. Even though the oxidation chemistry of ethylene has been studied extensively in the past, reports on the behavior at high pressure are sparse [1]. In particular, there is little knowledge about the interaction of ethylene with nitrogen oxides at elevated pressure. The presence of nitrogen oxides, even in small amounts, may have a significant impact on fuel oxidation characteristics [2]. Studies at atmospheric pressure [3-5] have revealed a mutual sensitization of the oxidation of NO_x and C_2H_4; a result of interactions of NO_x with the radical pool and with stable species. Under reducing conditions, C_2H_4 has the capacity to reduce NO to cyanide and amine species, mainly through the HCCO+NO reaction. This chemistry has been studied at atmospheric pressure, both experimentally and by chemical kinetic modeling [6-10].

To our knowledge, interactions of C_2H_4 and NO have not previously been studied at increased pressure, despite its relevance for, e.g., engines and gas turbines. The objective of the present work is to determine the effect of pressure on the mutual oxidation of C_2H_4 and NO, as well as evaluate the capability of ethylene to reduce NO under high pressure conditions and temperatures below 1000 K. The work involves an experimental and kinetic modeling study, analyzing the influence of the temperature and the oxygen content as the most relevant parameters for the C_2H_4/NO interaction. The results of the present work are compared to data from an earlier study on oxidation of C_2H_4 under similar high pressure conditions but in the absence of NO_x [1].

Experimental

The experiments of the C_2H_4-NO interaction have been carried out in a setup which consists of a laboratory-scale high pressure laminar flow reactor designed to approximate plug-flow. The installation is described in detail elsewhere [1, 11] and only a brief description is provided here.

The reactions take place in a tubular quartz reactor (i.d. 8 mm, o.d. 10 mm, lg. 1545 mm) enclosed in a stainless steel tube that acts as a pressure shell. A pressure control system consisting of two thermal mass flow pressure controllers automatically delivers N_2 to the shell-side of the reactor to obtain a pressure similar to that inside the reactor, thus avoiding devastating pressure gradients across the fragile quartz glass. The steel tube is placed horizontally in a tube oven with three individually controlled electrical heating elements that ensure an isothermal reaction zone (±5 K) of approximately 43 cm, with steep temperature gradients toward both the inlet and outlet of the reactor tube (Fig. 1). The reactor temperature is monitored by type K thermo-couples (±2.2 K or 0.75%) positioned in the void between the quartz reactor and the steel shell. Measured temperature profiles for the reactor have been reported elsewhere [11].

The reactant gases are premixed before entering the reactor. All gases used in the experiments are high purity gases or mixtures with certified concentrations (±2% uncertainty). The system is pressurized from the feed gas cylinders. The reactor pressure

is monitored upstream of the reactor by a differential pressure transducer and controlled by a pneumatic pressure valve positioned after the reactor, which is designed for steady state operation up to 60 bars. The reactant gas mixture contains 1000 ppm of C_2H_4 and 500 ppm of NO. The amount of O_2 is varied to obtain the desired stoichiometry for each experiment and the balance is made up with N_2. A total gas flow rate of 3000 mL (STP)/min is kept constant during the experiments, leading to a gas residence time as a function solely of the reaction temperature, t_r (s) = 8892/T [K].

Downstream of the reactor, the system pressure is reduced to atmospheric level through the pressure reduction valve prior to product analysis, which is conducted by a gas chromatograph, equipped with TCD and FID detectors, and a NO_x chemiluminescence gas analyzer. The GC allows detection of O_2, CO, CO_2, C_2H_6, C_2H_4, C_2H_2, and CH_4 with an overall relative measuring uncertainty in the range ±5%. A similar accuracy is obtained for measurements of NO and NO_2 using the NO_x chemiluminescence gas analyzer. The principle of the NO_2 measurement is by means of a catalytic converter that reduces NO_2 to NO by the use of a metal catalyst with a large surface area. However, HONO and $HONO_2$ are presumably converted to NO by the catalyst as well and thus we assume that the NO_2 measurement is in fact the sum of NO_2+HONO+$HONO_2$ concentrations. The entire downstream section is maintained at 395 K to avoid condensation of potential condensible components before product analysis. The diluted conditions ensure a low heat release during the reaction.

Chemical kinetic model

The experimental results have been analyzed in terms of a detailed chemical kinetic model for the oxidation of ethylene in the absence and presence of NO. The mechanism used for the modeling study, as well as the corresponding thermodynamic properties, was drawn from previous high-pressure work on conversion of $CO/H_2/O_2/NO_x$ [11], $CH_4/C_2H_6/O_2$ [12], and $CH_4/O_2/NO_x$ [13]. Recently, it was updated to describe C_2H_4 oxidation at high pressure, with particular emphasis on a number of oxygenated C_2-species important under low-temperature conditions [1]. In the present work, the subset describing the hydrocarbon/NO_x interactions was examined. Table 1 lists thermodynamic properties for selected components, while Table 2 lists key reactions in the C_2H_4-NO oxidation scheme. The full mechanism is available as Supplemental Material. Surface reactions were not included in the model. Our previous work on CH_4 oxidation [12] indicated loss of peroxides, but the similar work on C_2H_4 [1] showed no evidence of surface reactions. Either way, surface loss of peroxides would be minimized under the present conditions since they are rapidly removed by reaction with NO.

As the high pressure and intermediate temperature C_2H_4 oxidation has already been discussed in a previous study [1], the present focus is on the C_2H_4-NO_x interactions at similar conditions. The presence of NO_x introduces additional initiation steps for ethylene, with a smaller barrier than the C_2H_4+O_2 reaction. A direct reaction between C_2H_4 and NO_2 forms C_2H_3 and either HONO (R2b) or HNO_2 (R3b). Also addition is

possible (R1) [15], but the formed adduct dissociates rapidly back to reactants. In the absence of direct measurements of k_{2b} and k_{3b}, we have applied estimates for the reverse steps by analogy to the corresponding reactions of CH_3 [22]. After initiation, the major oxidation path for C_2H_4 involves the reaction sequence $C_2H_4 + OH \rightleftharpoons CH_2CH_2OH$, $CH_2CH_2OH + O_2 \rightleftharpoons HOCH_2CH_2OO$ [1]. Whereas the $HOCH_2CH_2OO$ peroxide was reported mainly to undergo thermal dissociation to $CH_2O + CH_2O + OH$ during pure C_2H_4 oxidation [1], the presence of NO opens up an oxidation path through the fast $HOCH_2CH_2OO$+NO reaction (R12). Due to the lack of measured values for k_{12}, the rate constant is estimated by analogy to the reaction between C_2H_5OO and NO.

There are a number of reactions taking place that recycle NO and NO_2 directly or through intermediate formation and subsequent decomposition of HNO_2, HONO, and $HONO_2$ [11]. Apart from formation of HONO and $HONO_2$, radicals such as CH_3, C_2H_3, C_2H_5, CH_2CHO, CH_3CO, and CH_2CH_2OH may conceivably take out NO_x. The CH_3+NO_x and C_2H_5+NO_x reactions, except for C_2H_5+NO [23], were drawn from Rasmussen et al. [13]. In the present work, we have added a number of reactions between hydrocarbon radicals and nitric oxide to the reaction mechanism, i.e. $C_2H_3 + NO$ (R4), $CH_2CHO + NO$ (R7), $CH_3CO + NO$ (R9), and $CH_2CH_2OH + NO$ (R10). Rate constants for most of these steps have been measured experimentally, though only in a limited pressure and temperature range, and extrapolation to the present conditions is uncertain. For the similar reactions involving NO_2 (R5, R6, R8, R11), rate constants are mostly estimates.

Thermodynamic properties for the formed adducts were estimated in the present work (Table 1). Optimized structures and vibrational frequencies (scaled by a factor of 0.99) for hydrocarbon radicals, NO, NO_2 and the adducts were obtained with B3LYP/6-311G(d,p) calculations. Energies were obtained via the CBS-QB3 approach of Petersson and coworkers [24], which approximates coupled cluster theory extrapolated to the complete basis set limit. These data yield the bond dissociation enthalpies of the adducts, which were combined with the thermochemistry of NO, NO_2 and the radicals [14] to obtain the enthalpies of formation of the adducts. The temperature-dependent entropies and heat capacities were derived from the moments of inertia and the frequencies via the rigid-rotor harmonic-oscillator approximation. For most of these components, data on the thermodynamic properties in literature are scarce. However, our calculated heat of formation for C_2H_3NO agree with the recent value by Klippenstein and coworkers ([25], personal communication) within 0.5 kcal/mol.

The subset involving reactions between the vinyl radical and nitrogen oxides warrants particular attention in the present work. There are a number of studies on the C_2H_3 + NO reaction [17, 25-29]; several of them focusing on the inhibiting role of NO in the pyrolysis of acetylene [26-28]. Recent experimental and theoretical results [17, 25] indicate that HCN + CH_2O (R4) is the only significant product channel near room temperature and at low pressure. Under the present conditions, we expect the reaction to proceed close to the high-pressure limit. Under these conditions, stabilization of nitrosoethylene (C_2H_3NO) might be expected, and presumably the fate of this component is important for forming reduced nitrogen species under the current conditions. We have

included a full reaction subset for C_2H_3NO, with rate constants estimated by analogy to the corresponding reactions of CH_3NO [22]. However, with the current thermochemistry for C_2H_3NO (Table 1), the thermal stability of this component is too low to facilitate reaction with other species. Instead C_2H_3NO dissociates rapidly, either back to reactants (C_2H_3 + NO) or to HCN + CH_2O. The barrier to form HCN + CH_2O is about 37 kcal/mol [25], 15 kcal/mol less than the barrier to C_2H_3 + NO. In the present work we have assumed that HCN + CH_2O is the sole product of the C_2H_3 + NO reaction, adopting the estimated high pressure limit at 700 K from Striebel et al. [17].

Studies of the C_2H_3+NO_2 reaction are scarce in literature. Geppert et al. [18] identified NO as the only reaction product observed for the vinyl radical reaction with NO_2 (R5). An attack of the vinyl radical on the N-atom site of NO_2 was suggested to be dominant; the nitroethylene formed could undergo isomerization to vinyl nitrite and subsequently eliminate NO and form the vinyloxy radical (CH_2CHO). Some stabilization of nitroethylene would be expected under the present conditions. The thermal dissociation of $C_2H_3NO_2$ has been studied theoretically [30, 31], but no rate constants have been reported. We have assumed that the C_2H_3+NO_2 recombination reaction (R6) proceeds with an estimated rate constant of 10^{13} cm^3 $mole^{-1}$ s^{-1}.

A calculation at 60 bar and 800 K for the nitrogen adducts with the current thermodynamic properties and dissociation/association kinetics indicates that the nitro species CH_3NO_2, $C_2H_3NO_2$, and $C_2H_5NO_2$, as well as the nitroso compounds CH_3NO, C_2H_5NO, and $CH_3C(O)NO$, have a much higher thermal stability than species such as

C_2H_3NO, $ONCH_2CH_2OH$, and $ONCH_2CHO$. It appears that reactions of NO with C_2 radicals such as C_2H_3, CH_2CHO, and CH_2CH_2OH, that may attain considerable concentrations under the present conditions, form adducts with a short lifetime, limiting their importance for removing NO.

Results and discussion

The interaction between C_2H_4 and NO, at concentrations of 1000 and 500 ppm, respectively, has been studied at 60 bar in the 600-900 K temperature range. In addition to temperature, the influence of the excess air ratio ranging from very fuel-rich (λ=0.2) to very fuel-lean conditions (λ=20) has been analyzed. The numerical predictions were obtained using the Plug Flow Reactor model of the CHEMKIN–PRO software [32].

Figure 2 compares experimental and modeling results at reducing conditions, whereas data sets obtained at stoichiometric and oxidizing conditions are presented in Figs. 3 and 4, respectively. In each case, the top graph represents the major carbon species concentration profiles (C_2H_4, CO, and CO_2), whereas the bottom graph shows the behaviour of the nitrogen oxides. Formation of HONO and $HONO_2$ is favoured by the high pressure of the present work, but presumably these species cannot be distinguished from NO_2 by the chemiluminescence analyzer used in the present study. In the figures, predicted NO_2 is shown as dashed lines, while HONO + $HONO_2$ + NO_2 are shown as solid lines.

It should be noted that a significant fraction of the fed NO is oxidized to NO_2 at low temperatures (600 K) prior to the C_2H_4 oxidation onset, even at reducing conditions. The conversion of NO to NO_2 is facilitated by the high pressure, low temperature, and the presence of O_2; conditions that favour the reaction $NO + NO + O_2 \rightleftharpoons NO_2 + NO_2$. This reaction may occur both in the inlet and outlet sections of the reactor. Consequently, all sections where the mixture is found at high pressure need to be included for an accurate modeling prediction of NO_x. The simulations range from the mixing point for NO and O_2 prior to the reactor to the pressure reduction valve after the reactor where the pressure is reduced to atmospheric level. The entire temperature profile used as model input, based on measurements from [11], is shown in Fig. 1. It is observed in the graphs that the model predicts accurately the NO and NO_2 concentration values at the lowest temperature of study for all stoichiometries except for oxidizing conditions, where the NO-to-NO_2 conversion is overpredicted.

Under reducing conditions (Fig. 2), C_2H_4 is converted mainly to CO and CO_2, with minor amounts (< 25 ppm) of C_2H_6 and CH_4 detected at the highest temperatures. Once oxidation of C_2H_4 is initiated, around 675 K, the NO_2 formed in the inlet section is reduced to NO. At 700 K and above, NO is further consumed and the observed total NO_x concentration is reduced about 20-25% compared to the inlet level.

The modeling predictions are generally in good agreement with the experimental results. The conversion of C_2H_4 to CO and CO_2, as well as the reduction of NO_2 to NO, is described well. However, while the model predicts well the reduction of NO at the high

temperature end, it is not able to capture the removal of NO_x observed at temperatures of about 700-850 K.

Under stoichiometric and oxidizing conditions (Figs. 3 and 4), the onset of oxidation is shifted to lower temperatures, 625-650 K. The CO concentration peaks about 75 K above the onset temperature. Again, the fuel oxidation behaviour is well predicted by the model. However, for both conditions the observed CO maximum is somewhat larger and appears at higher temperatures than the model predictions.

Under stoichiometric conditions (Fig. 3), the inlet NO_2 is gradually reduced to NO with increasing temperature, while the higher availability of O_2 under oxidizing conditions (Fig. 4) leads to NO_2 as the main NO_x compound. The NO/NO_2 partitioning is well predicted under stoichiometric conditions, even though total NO_x is slightly underpredicted at higher temperatures. Under oxidizing conditions, the model predicts correctly that NO above 700 K is largely oxidized to NO_2. The discrepancy observed at 600-700 K is attributed to an overprediction of.the NO-to-NO_2 conversion in the reactor inlet and heating section. However, it is noteworthy that the model predicts that a considerable fraction of the NO_x in this temperature range is present as HONO and $HONO_2$, rather than NO_2. Since the conversion efficiency of the analyzer catalyst for reducing HONO and $HONO_2$ to NO is presently unknown, there is some experimental uncertainty.

Except for the observed NO_x reduction above 700 K under reducing and stoichiometric conditions, the modeling predictions are in good agreement with the experimental results. This indicates that the important features of the chemistry are captured by the model. Figure 5 provides an overview of the most important oxidation pathways for C_2H_4 in the presence of NO, according to the model. For all the stoichiometries studied, the main consumption of C_2H_4 occurs through its reaction with OH to form CH_2CH_2OH. Hydroxyethyl mainly recombines with O_2 to form hydroxyethyl peroxide and minor amounts of ethanol, even though under stoichiometric and reducing conditions also the reaction with NO_2 (R11) is important. The $HOCH_2CH_2OO$ radical reacts with NO producing CH_2OH, CH_2O and NO_2 (R9) and to lesser extent it undergoes thermal dissociation. Under oxidizing conditions, reaction with HO_2 can also contribute to the $HOCH_2CH_2OO$ consumption. The intermediates formed by these reactions lead to the formation of CO and CO_2 as the main final products of the C_2H_4 combustion, through a reaction pathway involving CH_2O and HCO.

A smaller oxidation pathway for C_2H_4 involves C_2H_3, which is oxidized further by reaction with O_2 and NO_x. This oxidation pathway allows formation of HCN, along with small amounts of CH_3NO_2. Under reducing conditions, the oxygen availability is decreased, and atomic hydrogen becomes more important as a chain carrier. These conditions favour a smaller oxidation pathway through C_2H_5. The ethyl radical reacts with NO_2 to form nitro-ethane. In the higher end of the temperature range, C_2H_5 also reacts with formaldehyde to produce C_2H_6, which explains the small amount of C_2H_6 detected experimentally. A minor fraction of the ethyl radicals feed into the C_1

hydrocarbon pool to yield CH_4, as was observed under reducing conditions. Some of the methyl radicals formed through this pathway contribute to the formation of nitro-methane.

The major oxidation pathways of N-species derived from the model under the present conditions are shown in Figure 6. As the C_2H_4 oxidation takes place, NO and NO_2 react with the radical pool to form a number of N-containing intermediates, mainly HONO and $HONO_2$, and, to a lesser extent, HCN, $C_2H_5NO_2$ and CH_3NO_2. HONO is formed mainly by the CH_2O+NO_2 reaction, and under oxidizing conditions, also by reaction of NO_2 with HO_2. Subsequently it is consumed, mainly by its self reaction. $HONO_2$ is formed entirely by the NO_2+OH addition. Since $HONO_2$ consumption reactions are generally slow according to the model, this compound tends to accumulate until it dissociates thermally at higher temperatures.

The C_2H_3 + NO reaction (R4) can explain the removal of NO under reducing conditions above 850 K, where the vinyl radical is formed in larger quantities. However, the model does not capture the observed NO_x reduction in the 700-850 K range. Due to limitations in the measurement equipment, we were unable to detect any N-intermediates and thus it is not possible to conclude on the NO_x reduction trend. However, Rasmussen et al. [13] recently reported a similar reduction in NO_x for the $CH_4/O_2/NO_x$ system, increasing with pressure from 20 to 100 bar. The observed pressure dependence could indicate that the NO removal is initiated by formation of a thermally stable adduct. However, formation of nitro-hydrocarbons ($C_2H_3NO_2$, CH_3NO_2, $C_2H_5NO_2$) is limited by the low NO_2

concentration under the reducing conditions of Fig. 2 and, according to the model, the nitroso compounds (C_2H_3NO, CH_3NO, C_2H_5NO, $CH_3C(O)NO$, $ONCH_2CH_2OH$, $ONCH_2CHO$) are either not sufficiently stable above 700 K or formed in too small quantities to take out significant amounts of NO_x. The uncertainty in the thermodynamic properties of the nitro and nitroso compounds is limited and cannot explain the shortcoming in the modelling predictions. Further work is required to resolve this issue.

Figure 7 compares the experimental results of our previous study [1] with the present work, to show the influence of the presence of NO_x on C_2H_4 oxidation at high pressure. The high pressure facility and the experimental conditions are the same as in the current work, except for the absence of NO_x in the reactant mixture. In the absence of NO_x, the initiation of reaction occurs at about 750 K, independent of stoichiometry. The presence of NO_x shifts the onset of reaction 75-150 K to lower temperatures, the shift increasing with an increase in the availability of oxygen. For stoichiometric and oxidizing conditions, a complete conversion of C_2H_4 is attained, while under reducing conditions, independently of the presence of NO_x, almost 60% of the initial C_2H_4 is still unreacted at the highest temperature studied.

The present study confirms the mechanism of sensitization proposed by Doughty et al. [3]. They identified the major reaction pathway for oxidation of ethylene at atmospheric conditions and temperatures below 850 K and/or high [O_2] to involve OH addition to ethylene and subsequent reaction of the hydroxyethyl radical (CH_2CH_2OH), which involves a complex set of reactions in partial equilibria. If NO is present, it reacts fast

with the peroxide adduct (R12), pushing the system of equilibria towards products. However, in the absence of NO, the addition of OH to ethylene is close to equilibrium and products are formed only slowly through reactions of the hydroxyethyl radical. The higher pressures and longer reaction times of the present work push the chemistry towards lower temperatures, but the mechanism is the same as identified by Doughty et al.

Conclusions

An experimental and chemical kinetic study of the interaction between C_2H_4 and NO has been carried out under flow reactor conditions in the intermediate temperature range (600-900 K) and high pressure (60 bar), varying the stoichiometry from very fuel-rich (λ=0.2) to fuel-lean (λ=20). The mutual sensitization of C_2H_4 and NO_x, as well as the ability of C_2H_4 to remove NO under reducing conditions, has been investigated. A comparison with our earlier high pressure work on the C_2H_4/O_2 system [1] shows that the presence of NO_x shifts the onset of reaction 75-150 K to lower temperatures, the shift increasing with an increase in the availability of oxygen. Under reducing conditions and temperatures above 700 K, a significant fraction of the NO_x is removed, up to 28% compared to the inlet level.

Modeling predictions with a detailed chemical kinetic model are generally in good agreement with the experimental results, except under reducing conditions where the observed removal of NO_x is not explained by the model. The mechanism of sensitization

for the mutual oxidation of C_2H_4 and NO is attributed to the ability of NO to react rapidly with peroxides. The major oxidation path for C_2H_4 involves the reaction sequence C_2H_4 $+OH \rightleftharpoons CH_2CH_2OH$, $CH_2CH_2OH + O_2 \rightleftharpoons HOCH_2CH_2OO$. The presence of NO facilitates conversion of the peroxide through the reaction $HOCH_2CH_2OO + NO \rightarrow CH_2OH + CH_2O + NO_2$, pushing the system of partial equilibria towards products. This is a confirmation of the findings of Doughty et al. [3] for a similar system at atmospheric pressure.

A number of possibilities for removal of NO under reducing conditions has been investigated. The reaction $C_2H_3 + NO \rightarrow HCN + CH_2O$ is active in removing NO above 850 K. However, a second removal mechanism is active in the 700-850 K range, which is currently not identified. With the present thermochemistry and kinetics, neither formation of nitro-hydrocarbons (CH_3NO_2, $C_2H_3NO_2$, $C_2H_5NO_2$, $CHOCH_2NO_2$) nor nitroso-compounds (CH_3NO, C_2H_3NO, C_2H_5NO, $ONCH_2CHO$, $CH_3C(O)NO$, $ONCH_2CH_2OH$) contributes to remove NO_x.

Acknowledgements

The work is part of the CHEC (Combustion and Harmful Emission Control) research program. It was financially supported by the Technical University of Denmark and the Danish Technical Research Council. The authors would also like to express their gratitude to Ministerio de Ciencia e Innovación (MICINN) through project CTQ2006-

09963, for financial support. Mr. J. Giménez-Lopez acknowledges the MICINN for the pre-doctoral grant awarded.

References

[1] J.G. López, C.L. Rasmussen, M.U. Alzueta, Y. Gao, P. Marshall, P. Glarborg, *Proc. Combust. Inst.* 32 (2009) 367-375.

[2] P. Glarborg, *Proc. Combust. Inst.* 31 (2007) 77-98

[3] A. Doughty, F.J. Barnes, J.H. Bromly, B.S. Haynes, *Proc. Combust. Inst.* 26 (1996) 589-596

[4] M. Hori, N. Matsugana, N.M. Marinov, J.W. Pitz, C.K. Westbrook, *Proc. Combust. Inst.* 27 (1998) 389-396.

[5] P. Dagaut, O. Mathieu, A. Nicolle, G. Dayma, *Combust. Sci. Technol.* 177 (2005) 1767-1791.

[6] R. Bilbao, A. Millera, M.U. Alzueta, L. Prada, *Fuel* 76 (1997) 1401-1407.

[7] P. Glarborg, M.U. Alzueta, K. Dam-Johansen, J.A. Miller, *Combust. Flame* 115 (1998) 1-27.

[8] L. Prada, J.A. Miller, *Combust. Sci. Technol.* 132 (1998) 225-250.

[9] P. Dagaut, F. Lecomte, S. Chevailler, M. Cathonnet, *Combust. Flame* 119 (1999) 494-504.

[10] J. Giménez, M.P. Ruiz, A. Callejas, A. Millera, R. Bilbao, M.U. Alzueta, *Proc. 19th Int. Symp. Gas Kinetics* (2006) 247-248.

[11] C.L. Rasmussen, J. Hansen, P. Marshall, P. Glarborg, *Int. J. Chem. Kinet.* 40 (2008) 454–480.

[12] C.L. Rasmussen, J.G. Jacobsen, P. Glarborg, *Int. J. Chem. Kinet.* 40 (2008) 778-807.

[13] C.L. Rasmussen, A.E. Rasmussen, P. Glarborg, *Combust. Flame* 154 (2008) 529-545

[14] A. Burcat, B. Ruscic, *Third Millennium Ideal Gas andCondensed Phase Thermochemical Database for Combustion with Updates from Active Thermochemical Tables,* Report TAE960, Technion Israel Inst. of Technology, 16th September 2005.

[15] J.L. Sprung, H. Akimoto, J.N. Pitts Jr., J. A. Chem. Soc. 96 (1974) 6549-6554

[16] S. Gersen, A.V. Mokhov, J.H. Darmeveil, H.B. Levinsky, P. Glarborg, Ignition-promoting effect of NO_2 on methane, ethane and methane/ethane mixtures in a rapid compression machine, Proc. Combust. Inst., submitted for publication

[17] F. Striebel, L.E. Jusinski, A. Fahr, J.B. Halpern, S.J. Klippenstein, C.A. Taatjes, *Phys. Chem. Chem. Phys.* 6 (2004) 2216-2223.

[18] W.D. Geppert, A.J. Eskola, R.B. Timonen, L. Halonen, *J. Phys. Chem. A* 108 (2004) 4232-4238.

[19] D. Gutman, H.H. Nelson, *J. Phys. Chem.* 87 (1983) 3902-3905.

[20] J. Sehested, L.K. Christensen, O.J. Nielsen, T.J. Wellington, *Int. J. Chem. Kinet.* 30 (1998) 913-921.

[21] A. Miyoshi, H. Matsui, N. Washida, *Chem. Phys. Lett.* 160 (1989) 291-294.

[22] A.M. Dean, J.W. Bozzelli, *Combustion chemistry of nitrogen*, Chapter 2, in: W.C. Gardiner (Ed.), Gas Phase Combustion Chemistry, Springer-Verlag, New York, 2000.

[23] G. Pratt, I. Veltman, *J. Chem. Doc. Faraday Trans.* 72 (1976) 1733-1737.

[24] J.A. Montgomery Jr., M.J. Frisch, J.W. Ochterski, G.A. Petersson, J. Chem. Phys., 110 (1999) 2822.

[25] P. Zou, S.J. Klippenstein, D.L. Osborn, *J. Phys. Chem. A* 109 (2005) 4921-4929.

[26] A.G. Sherwood, H.E. Gunning, *J. Phys. Chem*. 69 (1965) 1732-1736.

[27] H. Ogura, *Bull. Chem. Soc. Japan* 51 (1978) 3418-3425.

[28] S.W. Benson, *Int. J. Chem. Kinet*. 26 (1994) 997-1011.

[29] W.H. Feng, B.S. Wang, H. Wang, F. Kong, *Acta Phys.-Chim. Sinica* 16 (2000) 776-778.

[30] A. Gindulyte, L. Massa, L.L. Huang, J. Karle, *J. Phys. Chem. A* 103 (1999) 11040-11044.

[31] A.G. Shamov, E.G. Nikolaeva, G.M. Khrapkovskii, *Russ. J. Gen. Chem.* 74 (2004) 1227-1242.

[32] Chemkin-PRO. Reaction Design, Inc., San Diego, CA 92121

Table 1. Thermodynamic properties of selected species in the reaction mechanism. Units are kcal mol^{-1} for H, and cal mol^{-1} K^{-1} for S and C_p. Temperature (T) range is in K.

Species	H_{298}	S_{298}	Cp_{298}	Cp_{400}	Cp_{500}	Cp_{600}	Cp_{800}	Cp_{1000}	Cp_{1500}	Ref.
C_2H_5NO	10.08	70.43	17.40	21.33	24.92	28.02	32.93	36.54	40.07	pw
CH_3CHNO	27.59	68.99	16.59	20.02	23.04	25.66	29.82	32.82	37.45	pw
C_2H_3NO	39.50	65.82	15.19	18.38	21.10	23.34	26.72	29.13	32.76	pw
CHCHNO	100.37	67.35	15.65	18.25	20.30	21.94	24.32	25.96	28.44	pw

$ONCH_2CHO$	3.75	73.90	18.59	22.16	25.23	27.80	31.71	34.47	38.49	pw
$ONCH_2CH_2OH$	-12.97	73.71	20.49	25.28	29.44	32.90	38.16	41.92	47.62	pw
$C_2H_5NO_2$	-24.81	76.59	18.97	23.50	27.65	31.23	36.58	40.45	45.84	[14]
$CH_2CH_2NO_2$	26.13	77.80	20.43	24.63	28.13	31.03	35.42	38.50	43.22	pw
$C_2H_3NO_2$	7.95	71.81	17.68	21.61	25.03	27.83	31.66	34.27	37.69	[14]
$CHCHNO_2$	69.90	72.53	17.85	21.24	23.91	26.02	29.02	31.01	33.94	pw
$CHOCH_2NO_2$	-41.20	78.65	20.72	25.05	28.71	31.77	36.37	39.47	44.00	pw
$CH_3C(O)NO$	-10.87	76.26	19.59	22.89	25.71	28.11	31.81	34.47	38.44	pw

Table 2. Selected reactions from the C_2H_4-NO high pressure subset. Parameters for use in the modified Arrhenius expression $k = AT^b\exp(-E/[RT])$. Units are mol, cm, s, cal.

		A	n	E	Ref.
1.	$C_2H_4+NO_2 \rightleftharpoons CH_2CH_2NO_2$	9.4E11	0.000	14000	[15] est
2.	$C_2H_3+HONO \rightleftharpoons C_2H_4+NO_2$	8.1E05	1.870	5504	$k_{CH3+HONO}$, [16]
3.	$C_2H_3+HNO_2 \rightleftharpoons C_2H_4+NO_2$	8.1E05	1.870	4838	$k_{CH3+HNO2}$, [16]

4.	$C_2H_3+NO \rightleftharpoons HCN+CH_2O$	1.1E13	0.000	0	[17], b, see text
5.	$C_2H_3+NO_2 \rightleftharpoons CH_2CHO+NO$	7.7E14	-0.600	0	[18]
6.	$C_2H_3+NO_2 \rightleftharpoons C_2H_3NO_2$	1.0E13	0.000	0	est
7.	$CH_2CHO+NO \rightleftharpoons ONCH_2CHO$	1.5E13	0.000	0	[19]
8.	$CH_2CHO+NO_2 \rightleftharpoons CH_2CO+HONO$	2.0E15	-0.680	1430	[3]
9.	$CH_3CO+NO \rightleftharpoons CH_3C(O)NO$	1.5E14	0.000	0	[20]
10.	$CH_2CH_2OH+NO \rightleftharpoons ONCH_2CH_2OH$	1.6E13	0.000	0	[21]
11.	$CH_2CH_2OH+NO_2 \rightleftharpoons CH_2O+CH_2OH+NO$	7.0E12	0.000	0	[3]
12.	$HOCH_2CH_2OO+NO \rightleftharpoons CH_2OH+CH_2O+NO_2$	1.6E12	0.000	-755	$k_{C2H5OO+NO}$

a: 60 bar, 600-900 K; b: Estimate of k_∞, 700 K

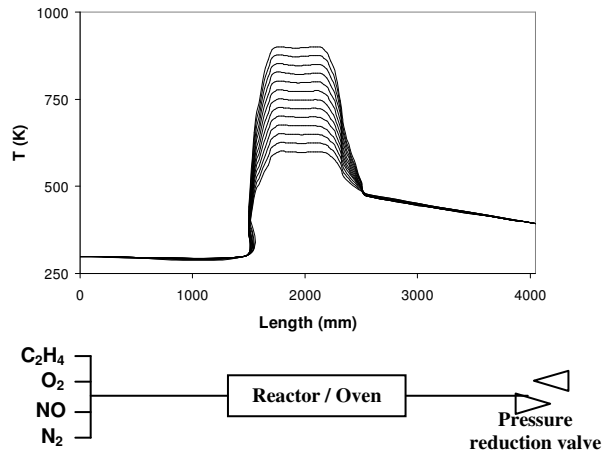

Figure 1. Temperature profiles provided for simulation in the CHEMKIN-PRO software [33]. The model input is divided in three regions. 1st region: From the mixing point of reactants to the entrance of the reactor, 1500 mm at 298 K. 2nd region: Reactor, 1050 mm at the measured temperature profiles in [11]. 3rd region: From the reactor outlet to the pressure reduction valve (1 atm), 1500 mm with a constant decrease of temperature down to 395 K.

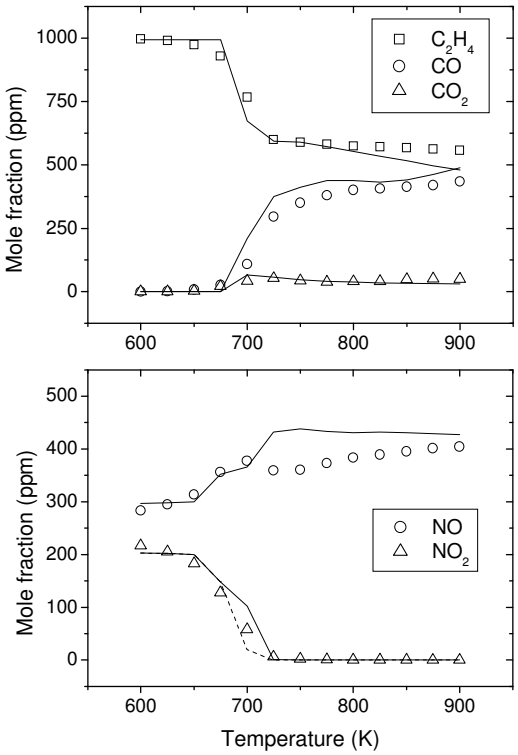

Figure 2: Comparison of experimental (symbols) and predicted concentration profiles (lines) as a function of the reactor temperature for the reducing experiment with $C_2H_4/O_2/NO$ (λ = 0.2). The inlet composition: 1000 ppm C_2H_4, 600 ppm O_2, 500 ppm NO; balance N_2. In the bottom graph, solid lines represent NO as well as the sum of NO_2+HONO+$HONO_2$, whereas dashed lines refer only to NO_2.

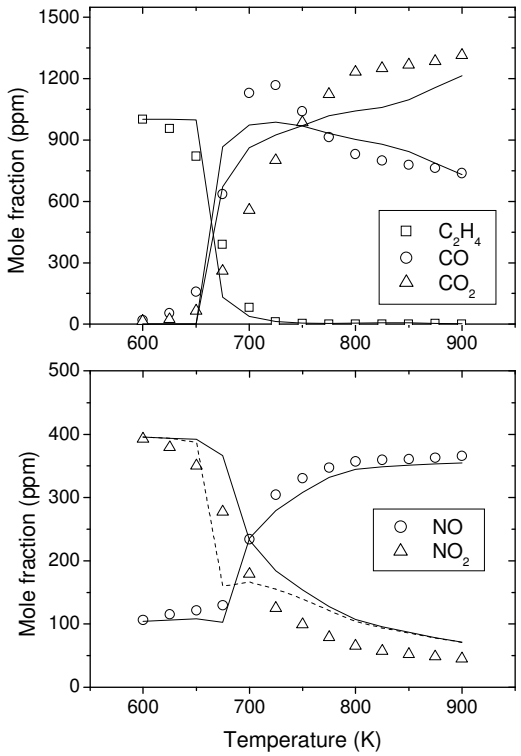

Figure 3: Comparison of experimental (symbols) and predicted concentration profiles (lines) as a function of the reactor temperature for the stoichiometric experiment with $C_2H_4/O_2/NO$ ($\lambda = 1$). The inlet composition: 1000 ppm C_2H_4, 3000 ppm O_2, 500 ppm NO; balance N_2. In the bottom graph, solid lines represent NO as well as the sum of NO_2+HONO+$HONO_2$, whereas dashed lines refer only to NO_2.

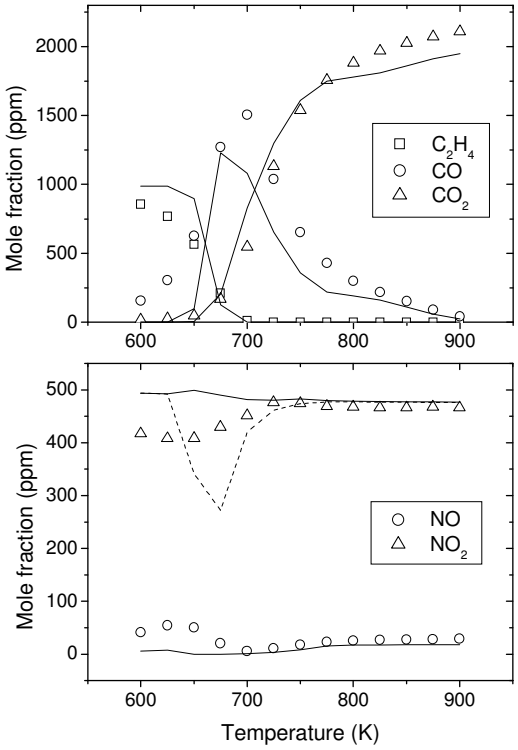

Figure 4: Comparison of experimental (symbols) and predicted concentration profiles (lines) as a function of the reactor temperature for the oxidizing experiment with $C_2H_4/O_2/NO$ ($\lambda = 20$). The inlet composition: 1000 ppm C_2H_4, 60000 ppm O_2, 500 ppm NO; balance N_2. In the bottom graph, solid lines represent NO as well as the sum of NO_2+HONO+$HONO_2$, whereas dashed lines refer only to NO_2.

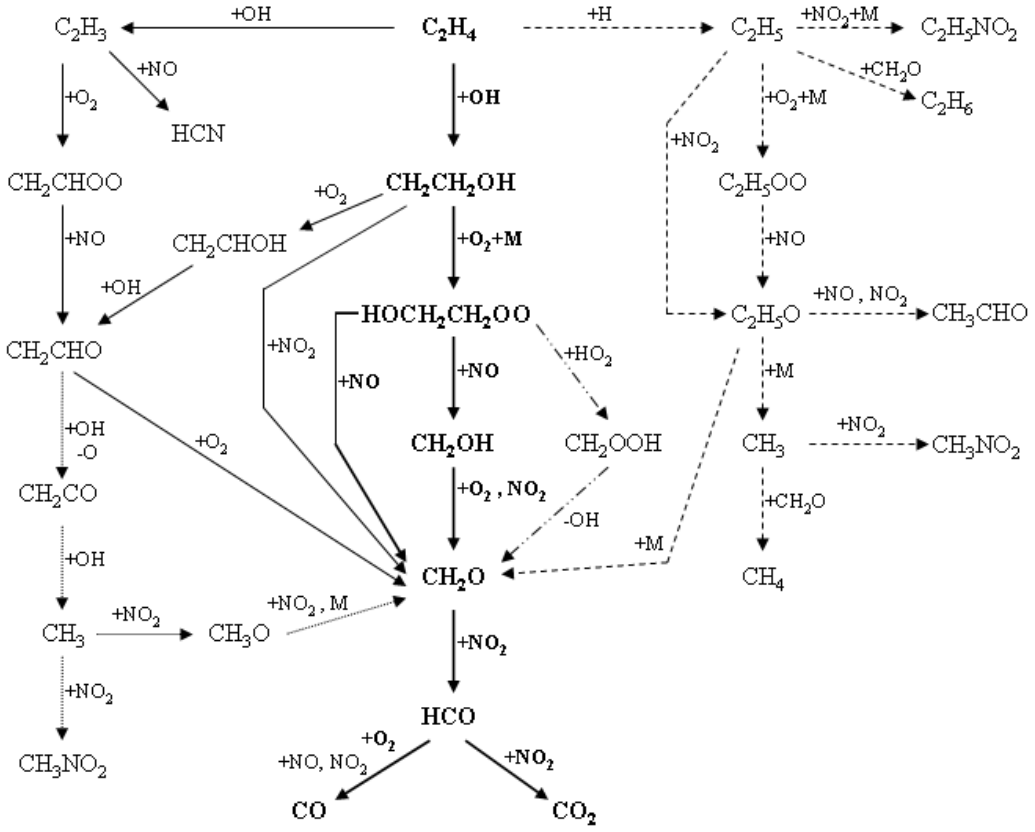

Figure 5: Main reaction pathways for C species in the C_2H_4/NO/O_2 interaction at the investigated conditions. The solid lines denote pathways important over the range of stoichiometries investigated, while dashed, dot and dash-dotted lines denote pathways important only under reducing-stoichiometric, reducing and oxidizing conditions respectively. The bold solid lines represent the main important pathway.

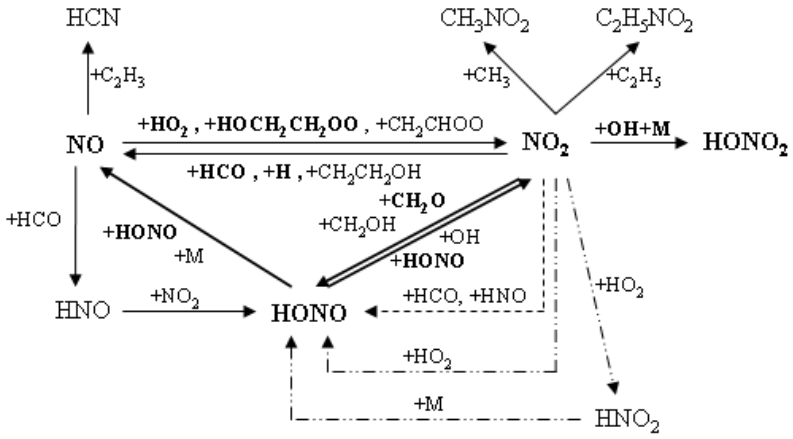

Figure 6: Main reaction pathways for N species in the C_2H_4/NO/O_2 interaction at the investigated conditions. The solid lines denote pathways important over the range of stoichiometries investigated, while dashed and dash-dotted lines denote pathways important only under reducing-stoichiometric and oxidizing conditions respectively. The bold solid lines represent the main important pathway.

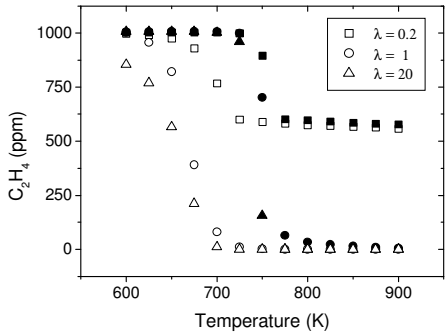

Figure 7: Experimental results of the C_2H_4 concentration as a function of the presence of NO and the stoichiometry: reducing (λ=0.2), stoichiometric (λ=1) and oxidizing conditions (λ=20). Solid symbols represent combustion without NO [1] and open symbols with the presence of a constant amount of 500 ppm of NO. Apart from the presence of NO, inlet composition, pressure, and residence time are the same for each stoichiometry.